

# The field-induced magnetic ordering transition in $\text{TlCuCl}_3$

Jesko SIRKER, Alexander WEISSE and Oleg P. SUSHKOV

*School of Physics, The University of New South Wales, Sydney 2052, Australia*

(Received June 20, 2018)

In the first part we investigate in detail if the Bose-Einstein condensation scenario for magnons can quantitatively explain the observed field-induced magnetic ordering in  $\text{TlCuCl}_3$ . We use a bond-operator approach to map the spin system onto hard-core bosons and exactly account for the hard-core constraint in the dilute limit. We solve the hard-core model within the Hartree-Fock-Popov approximation and discuss its validity and the consequences of this approximation for the critical properties. In the second part the effects of spin-phonon and spin-orbit coupling are discussed within this framework. We show that the experimental magnetization and specific heat data are well described if a certain type of anisotropy is included. We also present predictions for the quasiparticle gap which might be tested in the future.

KEYWORDS: Spin-gap systems, Bose-Einstein condensation,  $\text{TlCuCl}_3$

## 1. Introduction

Antiferromagnetic systems such as integer-spin chains, spin-1/2 ladders with an even number of legs or systems where the spins form a network of weakly coupled dimers share the common property that an excitation gap  $\Delta$  between the singlet ground state and the triplet state exists. An applied magnetic field  $H$  leads to a Zeeman splitting of the massive triplet with the lowest mode crossing the ground state at a critical field  $H_g = \Delta/g\mu_B$ . The ground state for  $H > H_g$  can be regarded as a Bose-Einstein condensate (BEC) of this bosonic mode<sup>1-3</sup>. This is particularly easy to understand for  $S = 1/2$  spins where the bond-operator (BO) representation

$$S_{1,2}^\alpha = \frac{1}{2}(\pm t_\alpha \pm t_\alpha^\dagger - i\epsilon_{\alpha\beta\gamma} t_\beta^\dagger t_\gamma) \quad (1)$$

of two neighbouring spins  $S_{1,2}$  in terms of bosonic triplet creation (annihilation) operators  $t_\alpha^\dagger$  ( $t_\alpha$ ) is exact<sup>4-6</sup>. Using (1) the spin-Hamiltonian can be mapped exactly onto a Hamiltonian in terms of the bosonic operators  $t_\alpha$ . The magnetic field  $H$  becomes the chemical potential  $\mu$  for the magnons and the concept of BEC is in principle directly applicable. Note, however, that the magnons are subject to the hard-core constraint  $t_{\beta i}^\dagger t_{\alpha i}^\dagger = 0$ , i.e., only one triplet is allowed at the bond  $i$ . The magnons therefore form an *interacting* Bose gas and the problem in terms of bosonic operators is in general as complicated as that in terms of the original spin operators. The BEC concept for the field-induced magnetic ordering in spin-gap systems becomes only helpful if the magnon density  $n$  is small. More precisely, the average distance between the magnons  $l \sim n^{-1/3}$  should be much larger than the s-wave scattering length  $a$  which is the characteristic length scale representing the influence of the repulsive potential. This implies that  $a/l \sim n^{1/3}a \ll 1$  so that the magnons have to be dilute. In this case the well-established gas approximation<sup>7</sup> which involves a systematic expansion in terms of the small parameter  $n^{1/3}a$  is applicable and even the finite temperature properties of the interacting Bose gas can be studied analytically<sup>8</sup>. In  $\text{TlCuCl}_3$  this situation is realized in magnetic fields

$H \sim 6 - 7$  T and this compound has therefore been studied extensively in recent years<sup>3,9-21</sup>. Inelastic neutron scattering (INS)<sup>11</sup> has revealed that  $\text{TlCuCl}_3$  has an excitation gap  $\Delta \approx 0.7$  meV in zero magnetic field and a bandwidth  $W \sim 6.3$  meV. The dimers in this compound are formed by the  $S = 1/2$  spins of neighbouring  $\text{Cu}^{2+}$  ions and weaker interdimer interactions are mediated by the  $\text{Cl}^-$  ions yielding a three dimensional dimer network. On the theoretical side it has been shown that the measured magnetisation curves can be qualitatively reproduced within the BEC picture<sup>3</sup>. In addition, the magnon dispersion has been described by using the BO formalism<sup>9</sup>. More recently we pointed out that anisotropies induced by spin-orbit coupling can influence BEC in spin-gap systems dramatically. Taking such anisotropies into account we have shown that for  $\text{TlCuCl}_3$  it is possible to obtain good quantitative agreement between the measured magnetisation curves and those calculated within the BEC framework<sup>15</sup>.

In the present paper we want to extend<sup>15</sup> with respect to the following aspects: In section 2 we will show how the hard-core constraint can be taken into account for dilute magnons beyond the mean-field level thus improving the results in Ref.<sup>9</sup>. In particular, this approach allows us to calculate the magnon-magnon scattering amplitude directly. In section 3 we will discuss the validity of the Hartree-Fock-Popov approximation (HFPA) which we use to solve the hard-core boson model. We will also investigate how this approximation affects the critical properties of the model. In section 4 we discuss the influence of crystal-field anisotropies for the BEC. We also investigate in more detail the case of a staggered  $g$  tensor and/or antisymmetric (Dzyaloshinsky-Moriya) spin interactions proposed in Ref.<sup>15</sup> to explain the measured magnetisation curves. In particular we will show results for different orientations of the magnetic field. In section 5 we compare the results of our theory for the specific heat with experimental data. The last section presents a summary and conclusions.

## 2. Bond-operator formalism

The BO technique starts from the strong coupling ground state  $|s\rangle$  where each dimer at bond  $i$  forms a singlet  $|i, s\rangle$ . The operators  $t_{i\alpha}^\dagger$  then create local triplet excitations  $|i, \alpha\rangle = t_{i\alpha}^\dagger |i, s\rangle$  with  $|i, +\rangle = -|\uparrow\uparrow\rangle$ ,  $|i, -\rangle = |\downarrow\downarrow\rangle$  and  $|i, 0\rangle = (|\uparrow\downarrow\rangle + |\downarrow\uparrow\rangle)/\sqrt{2}$ . For  $\text{TlCuCl}_3$  an effective Heisenberg-type Hamiltonian has been derived in<sup>9,10,12</sup> containing the intradimer coupling  $J$  and three interdimer couplings  $J_a, J_{a2c}, J_{abc}$ . In these works it has been argued that the exchange paths corresponding to these interdimer couplings are most important. This has been confirmed in a recent electronic structure calculation<sup>17</sup>. We have checked that including additional exchange paths which might be also of some relevance<sup>17</sup> does not significantly improve the results presented here. We therefore restrict ourselves to the model considered in<sup>9,10</sup>. Using (1) and retaining only terms bilinear in the triplet operators one easily derives<sup>9</sup>

$$H = \sum_{\mathbf{k}\alpha} \left\{ (A_{\mathbf{k}} + \alpha g \mu_B H) t_{\mathbf{k}\alpha}^\dagger t_{\mathbf{k}\alpha} + \frac{B_{\mathbf{k}}}{2} (t_{\mathbf{k}\alpha} t_{-\mathbf{k}\bar{\alpha}} + h.c.) \right\} \quad (2)$$

with  $A_{\mathbf{k}} = J + f_{\mathbf{k}} + g_{\mathbf{k}}$ ,  $B_{\mathbf{k}} = f_{\mathbf{k}} + g_{\mathbf{k}}$ ,  $f_{\mathbf{k}} = J_a \cos k_x + J_{a2c} \cos(2k_x + k_z)$ ,  $g_{\mathbf{k}} = 2J_{abc} \cos(k_x + k_z/2) \cos(k_y/2)$ ,  $\bar{\alpha} = -\alpha$  where  $-\pi \leq k_x, k_y \leq \pi$  and  $-2\pi \leq k_z \leq 2\pi$ . By the Bogoliubov transform  $t_{\mathbf{k}\alpha} = u_{\mathbf{k}} \tilde{t}_{\mathbf{k}\alpha} + v_{\mathbf{k}} \tilde{t}_{-\mathbf{k}, \bar{\alpha}}^\dagger$  the Hamiltonian gets diagonal with eigenvalues

$$\omega_{\mathbf{k}\alpha} = \sqrt{A_{\mathbf{k}}^2 - B_{\mathbf{k}}^2} - \alpha g \mu_B H \quad (3)$$

and Bogoliubov coefficients

$$u_{\mathbf{k}}^2, v_{\mathbf{k}}^2 = \pm \frac{1}{2} + \frac{A_{\mathbf{k}}}{2\omega_{\mathbf{k}0}}. \quad (4)$$

A good fit of the measured magnon dispersion<sup>11</sup> can be obtained from (3) using  $J, J_a, J_{a2c}, J_{abc}$  as fitting parameters. Because these parameters are not very sensitive to the gap value whereas the magnetic properties for fields  $H \gtrsim H_g$  crucially depend on  $\Delta$  we prefer to fix the gap and use it as a constraint in the fitting procedure. Results for  $\Delta = 0.65, 0.8$  and  $1.0$  meV are given to the left of each column in table I and are consistent with<sup>9</sup>.

Next we discuss the renormalization of the dispersion (3) due to the hard-core constraint. Following<sup>6</sup> this condition can be taken into account by introducing an infinite on-site repulsion between the bosons:

$$H_U = U \sum_{i, \alpha, \beta} t_{i\alpha}^\dagger t_{i\beta}^\dagger t_{i\alpha} t_{i\beta}, \quad U \rightarrow \infty. \quad (5)$$

The corresponding scattering vertex  $\Gamma_{\alpha\beta, \alpha\beta}(\mathbf{K})$  where  $\mathbf{K} = (\mathbf{k}, \omega)$  is the total momentum and energy of the incoming particles can be calculated exactly in the dilute limit by a summation of ladder diagrams. This yields

$$\Gamma(\mathbf{K}) = - \left( \frac{1}{N} \sum_{\mathbf{q}} \frac{v_{\mathbf{q}}^2 u_{\mathbf{k}-\mathbf{q}}^2}{\omega - \omega_{\mathbf{q}} - \omega_{\mathbf{k}-\mathbf{q}}} \right)^{-1}. \quad (6)$$

For magnetic fields  $H \gtrsim H_g$  only particles near the band minimum at  $\mathbf{q}_0 = (0, 0, 2\pi)$  are excited so that the energy and momentum dependent  $\Gamma(\mathbf{K})$  can be replaced by the constant  $v_0 = \Gamma(\mathbf{q}_0, 0)$ . Because  $u_{\mathbf{k}}^2$  is close to 1,

$v_0$  is approximately given by the magnon bandwidth  $W$ . However, it is known that the hard-core constraint (5) leads to a renormalisation of the Bogoliubov coefficients (4) and also to a renormalised triplet spectrum<sup>6</sup>

$$\Omega_{\mathbf{k}0} = Z_{\mathbf{k}} \sqrt{(A_{\mathbf{k}} + \Sigma_n(\mathbf{k}, 0))^2 - (B_{\mathbf{k}} + \Sigma_a)^2}. \quad (7)$$

Here  $Z_{\mathbf{k}}^{-1} = 1 - \partial \Sigma_n / \partial \omega$  is the quasiparticle residue,  $\Sigma_n(\mathbf{k}, \omega)$  the normal and  $\Sigma_a$  the anomalous self-energy. Values for these quantities and the renormalised superexchange parameters are given in brackets in table I. Although the superexchange parameters are considerably renormalised, the shape of the dispersion is only slightly changed because  $\Sigma_n, \Sigma_a$  and  $Z$  are almost momentum independent here and, in addition, a fit to the measured dispersion is performed. The most important consequence is a renormalisation of the scattering amplitude  $v_0$  by more than 20%. The dispersions for all 3 gap-values are shown in Fig. 1 in comparison to the INS-data. In all

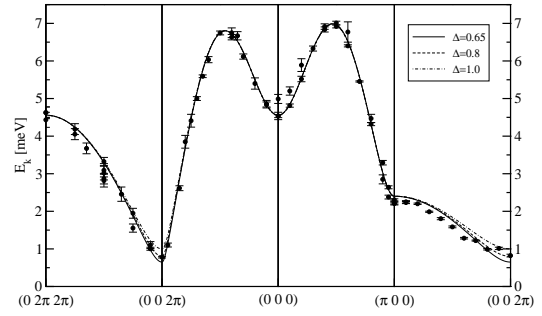


Fig. 1. Dispersion relation for  $\text{TlCuCl}_3$  measured by INS (circles)<sup>11</sup> in comparison to the theoretically calculated ones with fixed gap values  $\Delta = 0.65, 0.8, 1.0$  meV.

cases the experimental data are well described and differences between the 3 fits are only visible close to  $\mathbf{q}_0$ .

## 3. HFP approximation

As we are interested in temperatures  $T < \Delta \ll v_0$  we can treat  $v_0$  as temperature independent and it is also sufficient to take only the lowest triplet mode ( $\alpha = +$ ) into account. For simplicity we define  $\epsilon_{\mathbf{k}} \equiv \Omega_{\mathbf{k}0} - \Delta$ . The Hamiltonian for the lowest triplet mode is then given by

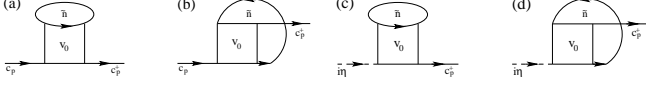
$$H = \sum_{\mathbf{k}} (\epsilon_{\mathbf{k}} - \mu_0) t_{\mathbf{k}}^\dagger t_{\mathbf{k}} + \frac{v_0}{2} \sum_{\mathbf{k}, \mathbf{k}', \mathbf{q}} t_{\mathbf{k}+\mathbf{q}}^\dagger t_{\mathbf{k}'-\mathbf{q}}^\dagger t_{\mathbf{k}} t_{\mathbf{k}'} \quad (8)$$

where  $\mu_0 = g \mu_B (H - H_g)$ . To allow for the symmetry breaking in the condensed phase we introduce new operators  $t_{\mathbf{k}} = c_{\mathbf{k}} + i \delta_{\mathbf{k}, \mathbf{q}_0} \eta$  where  $\eta$  is a real number and  $n_0 = \eta^2$  the condensate density. To diagonalise (8) we have to deal with the terms which are cubic or quartic in the new operators  $c_{\mathbf{k}}$ . The simplest way to treat these terms is the one-loop approximation which yields the Hartree and the Fock diagram for the quartic term (see Fig. 2). Therefore this approximation is often called Hartree-Fock-Popov approximation (HFPA). As a result we find  $H = H_c + H_{\text{lin}} + H_{\text{bilin}}$  where

$$H_c = \frac{v_0}{2} n_0^2 - \mu_0 n_0$$

Table I. Superexchange parameters, self-energies, scattering amplitude  $v_0$  and effective mass  $m$  for dispersion (3) and (7) (in brackets).

$\Delta$ [meV]	$J$ [meV]	$J_a$ [meV]	$J_{a2c}$ [meV]	$J_{abc}$ [meV]	$\Sigma_n$ [meV]	$\Sigma_a$ [meV]	$Z$	$v_0$ [meV]	$m$ [1/meV]
0.65	5.52 (4.83)	-0.24 (-0.30)	-1.57 (-1.84)	0.46 (0.58)	0 (1.24)	0 (0.46)	1 (0.91)	8.01 (9.91)	0.25 (0.26)
0.8	5.52 (4.77)	-0.23 (-0.29)	-1.56 (-1.82)	0.45 (0.57)	0 (1.25)	0 (0.45)	1 (0.91)	7.77 (9.44)	0.32 (0.32)
1.0	5.51 (4.78)	-0.21 (-0.27)	-1.56 (-1.81)	0.45 (0.55)	0 (1.20)	0 (0.43)	1 (0.92)	7.39 (8.89)	0.41 (0.42)

Fig. 2. (a), (b): Hartree and Fock diagram. (c), (d): Additional one-loop diagrams due to the terms cubic in  $c_{\mathbf{k}}^{(\dagger)}$ .

$$H_{\text{lin}} = i(2\tilde{n}v_0\eta + v_0n_0\eta - \mu_0\eta)(c_{\mathbf{q}_0}^\dagger - c_{\mathbf{q}_0}) \quad (9)$$

$$H_{\text{bilin}} = \sum_{\mathbf{k}} \left\{ \mathcal{A}_{\mathbf{k}} c_{\mathbf{k}}^\dagger c_{\mathbf{k}} - \frac{\Sigma_{12}}{2} (c_{\mathbf{k}}^\dagger c_{-\mathbf{k}}^\dagger + h.c.) \right\}$$

with  $\tilde{n}$  being the density of non-condensed magnons. Here  $\mathcal{A}_{\mathbf{k}} = \epsilon_{\mathbf{k}} - \mu_0 + \Sigma_{11}$  with the normal self-energy  $\Sigma_{11} = 2v_0\tilde{n} + 2v_0n_0$  and the anomalous self-energy  $\Sigma_{12} = v_0n_0$ . By a standard Bogoliubov transform  $H_{\text{bilin}}$  can be diagonalised and  $E_{\mathbf{k}} = (\mathcal{A}_{\mathbf{k}}^2 - \Sigma_{12}^2)^{1/2}$  is the quasiparticle spectrum. In addition  $H_{\text{lin}}$  has to vanish.

It is important to note that the HFPA is parametrically justified in the present case: The magnon density  $n = \tilde{n} + n_0$  is small and diagrams taken into account in the HFPA are the leading diagrams in a systematic expansion in  $n$ . However, when  $T \rightarrow T_c$  from below, where  $T_c$  is the critical temperature of the Bose gas, it is well known that the condensate density  $n_0$  in the HFPA does not vanish. Therefore the total density jumps and the HFPA falsely predicts a first order phase transition<sup>8</sup>. This is due to the fact that any perturbative approach fails at the critical point where the scale for fluctuations diverges. By estimating when the next-leading diagrams become as important as the diagrams taken into account one finds<sup>8</sup> that the HFPA is justified when

$$|T_c - T| \gg an^{1/3}T_c. \quad (10)$$

As  $an^{1/3}$  is our small parameter, the temperature region around the critical point where this perturbative approach is not justified is usually very small.

In many papers about BEC in  $\text{TlCuCl}_3$  much interest has focused onto the fact that  $H_c(T) - H_g \sim T^\phi$  with  $\phi \sim 2^3$  where  $H_c$  is the critical field where BEC occurs. This has led to a discussion why the ‘‘critical exponent’’  $\phi$  deviates from  $3/2$  which is the result within the HFPA provided that the magnon dispersion is quadratic. In the same way one can also consider  $n_c(T) \sim T^\phi$  and finds from the experimental data<sup>3</sup> that this ‘‘power law’’ yields a good fit with a similar exponent  $\phi \sim 2$ . In HFPA one finds  $n_c(T) \sim T^{3/2}$ . Therefore it has been speculated<sup>3,22</sup> that the HFPA fails, i.e., that the ‘‘critical exponent’’ is renormalised due to quantum fluctuations.

First, it is worth to note that we are dealing with quantities which are not dimensionless. Therefore the exponent is dictated by dimensional analysis. If the dispersion is given by  $\epsilon \sim k^\alpha$  we will find in  $d$ -dimensions that  $n_c(T) \sim T^{d/\alpha}$ . Of course, the proportionality factor is

not necessarily temperature independent as in the HFPA. But it can only depend on the dimensionless quantity  $aT^{1/\alpha}$  (or equivalently  $an^{1/3}$  which is small for a dilute gas) where the scattering length  $a$  is the only length scale in our problem. Corrections of this kind have indeed been found for interacting Bose gases<sup>23</sup>. As a consequence there is no longer a simple power law. However, for the BEC of magnons there is also another effect which makes a simple power law invalid even within HFPA: The dispersion is certainly quadratic for small excitation energies but the range of validity of the quadratic approximation might be rather small. As we pointed out<sup>15,16</sup> this is indeed the case for  $\text{TlCuCl}_3$  where the quadratic approximation is only justified for  $T < 1$  K which is well below the experimental temperature range<sup>3</sup>. To see this we show in Fig. 3  $n_c(T)$  calculated within the HFPA using the triplet dispersions from Fig. 1. Whereas for

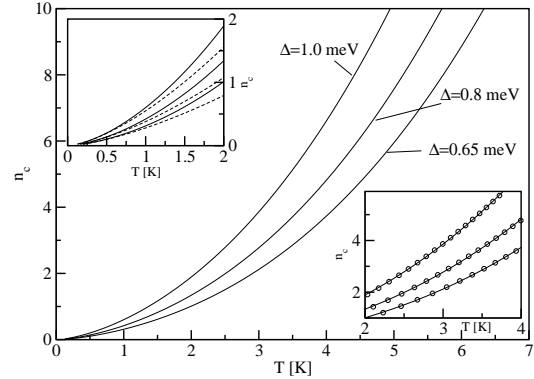


Fig. 3.  $n_c(T)$  within HFPA with dispersions from Fig. 1. Upper inset: For  $T < 1$  K the dispersions are almost quadratic and  $n_c \sim T^{3/2}$  (dashed lines). Lower inset:  $n_c(T)$  is well fitted by a ‘‘power law’’ (symbols) with exponents 1.92 ( $\Delta = 0.65$  meV), 1.88 ( $\Delta = 0.8$  meV) and 1.82 ( $\Delta = 1.0$  meV) for  $2 < T < 4$  K.

$T < 1$  K we indeed see that  $n_c \sim T^{3/2}$  there is no power law at higher temperatures. However, as shown in the lower inset of Fig. 3 it is still possible to obtain an excellent fit by a ‘‘power law’’ even at higher temperatures provided that the considered temperature range is sufficiently small. For the temperature range in<sup>3</sup> we find an exponent  $\phi \sim 1.8 - 1.9$  which is in good agreement with experiment and a recent work<sup>18</sup> where also a realistic dispersion has been used. We should not take this agreement too serious because the HFPA is not justified at the critical point. In addition, we will argue in the next section that anisotropies play a crucial role and that actually no phase transition occurs. What Fig. 3 nevertheless does show is that in the experimental temperature range  $n_c(T)$  does depend on microscopic details and no universal power law exists.

#### 4. Spin-phonon and spin-orbit coupling

In<sup>15</sup> we have shown that the magnetisation  $M(T)$  calculated with the dispersion (7) and  $v_0 \sim 10$  meV as obtained by the BO formalism does not fit the experimental data. However, our calculation of  $v_0$  in section 2 does only include magnon-magnon scattering. From Raman spectroscopy<sup>13</sup> and sound attenuation experiments<sup>14</sup> it is known that phonons are important. Because optical phonon modes exist at energies comparable with the energy scale of the magnetic excitations<sup>13</sup> it is not clear if the effect of magnon-phonon scattering can be calculated perturbatively. We have therefore used  $v_0$  as a fit parameter and obtained best agreement with experiment for  $v_0 \approx 25$  meV as shown in Fig. 4a. A renormalisation

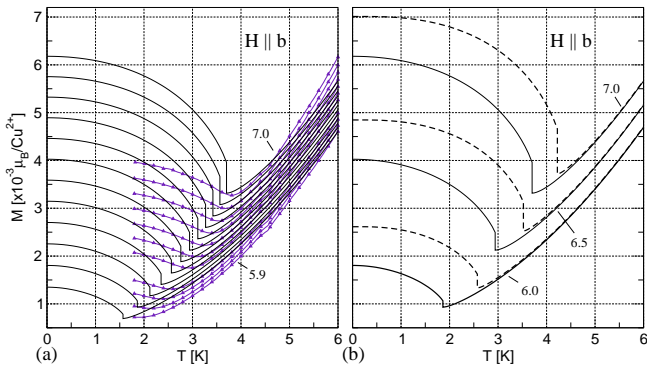


Fig. 4. (a) Experimental magnetisation curves (symbols) for  $H = 5.9, 6.0, \dots, 7$  T from Ref.<sup>3</sup> compared to the theoretically calculated (solid lines) with  $\Delta = 0.67$  meV,  $v_0 = 25$  meV. (b) Theoretical magnetisation curves as in (a) (solid lines) and with an additional exchange anisotropy  $\tilde{\gamma} = 0.01$  meV (dashed lines).

of  $v_0$  by a factor 2 – 3 might be caused by a reduction of the bare magnon bandwidth due to polaronic effects. But even with  $v_0 = 25$  meV we can obtain good agreement with experiment only for  $T > T_c$ . At low- $T$  our theory still overestimates  $M(T)$  by 50%.  $an^{1/3} \sim 0.1$  so that HFA should be justified according to (10) apart from a region  $\sim \pm 0.5$  K around the critical point. The approximation therefore cannot explain the failure of our theory at low- $T$ .

In any real magnetic system there is some kind of anisotropy which reduces the symmetry. In a system without magnetic field and anisotropies we have the usual  $SU(2)$  symmetry. By a magnetic field this symmetry is reduced to  $U(1)$  around the magnetic field axis. Spontaneous breaking of  $U(1)$  occurs at the BEC transition and is responsible for a gapless Goldstone mode in the phase with  $n_0 \neq 0$ . Any kind of anisotropy will in general break  $U(1)$  explicitly so that there is no longer a Goldstone mode. However, depending on the type of anisotropy there might be still a  $\mathcal{Z}_2$  symmetry (changing the sign of the triplet operator) so that a transition between a phase with and without condensed magnons is still possible. Finally, if the anisotropy breaks  $\mathcal{Z}_2$  no phase transition will occur and for a small symmetry breaking anisotropy we expect the phase transition to be smeared out to a crossover.

Here we want to discuss two kinds of anisotropy. First, we want to consider an exchange anisotropy (EA) within a dimer, i.e., we consider  $J \rightarrow \{J^x, J^y, J^z\}$ . Using triplet operators, performing the Bogoliubov transformation with parameters as in Eq. (4) and considering only the lowest triplet mode we find

$$H_{1,\text{pert}} = \tilde{\gamma}(t_{\mathbf{k}}t_{-\mathbf{k}} + t_{\mathbf{k}}^\dagger t_{-\mathbf{k}}^\dagger) \quad (11)$$

as perturbation to (8) where  $\tilde{\gamma} \propto J_x - J_y$ . This kind of perturbation can also originate from a “single-ion anisotropy” for the triplets  $\sim D(S_1^z + S_2^z)^2 + E[(S_1^x + S_2^x)^2 - (S_1^y + S_2^y)^2]$  where  $\mathbf{S}_{1,2}$  denote the spins within one dimer. On the other hand consider a Dzyaloshinsky-Moriya anisotropy (DMA)  $\sim \mathbf{D} \cdot (\mathbf{S}_1 \times \mathbf{S}_2)$  within the dimer. Transforming this type of interaction into triplet operators we find

$$H_{2,\text{pert}} = i\gamma(t_{\mathbf{q}_0} - t_{\mathbf{q}_0}^\dagger) \quad (12)$$

where the wave vector  $\mathbf{q}_0$  depends on how the DM-vector  $\mathbf{D}$  varies in space<sup>15</sup>. In particular we want to consider the case where  $\mathbf{q}_0$  corresponds to the minimum of the triplet dispersion. Both types of anisotropy yield additional contributions to the Hamiltonian (9) and results for the quasiparticle spectra and the additional constraints due to the linear term are given in table II. When compared to the case without anisotropy we see that the EA yields a small shift  $\tilde{\gamma}/v_0$  in  $n_c$  and also a small quasiparticle gap  $\Delta_{qp} = \sqrt{8\tilde{\gamma}v_0n_0}$  in the condensed phase. At the critical point,  $\Delta_{qp}$  is zero. Fig. 4b shows that apart from the shift in  $n_c$  the shape of the magnetisation curves is basically unaffected. On the other hand a DMA has a dramatic effect even if it is tiny because it smears out the phase transition to a crossover. As already shown in<sup>15</sup> it is possible to obtain excellent agreement with the measured magnetisation curves for  $H \parallel b$  when a DMA  $\gamma = 10^{-3}$  meV is included (see Fig. 5a). In an ideal  $\text{TiCuCl}_3$  crystal the centre of each dimer is an inversion centre.  $\gamma \neq 0$  therefore requires small lattice distortions. If these distortions are of such kind that  $\mathbf{D}$  is oriented along a specific direction throughout the crystal it would be possible to restore  $U(1)$  symmetry by applying the magnetic field along the same axis. In this configuration a sharp phase transition would still occur. We therefore compare here also with experimental results

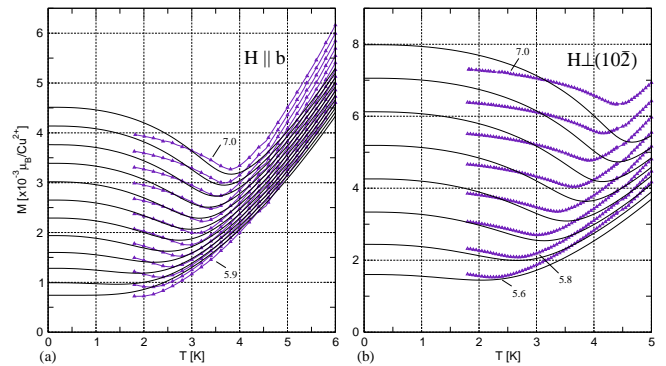


Fig. 5. (a): Experimental magnetisation curves as in Fig. 4a and theoretically calculated with  $g = 2.06^{19}$ ,  $\Delta = 0.72$  meV,  $v_0 = 27$  meV and  $\gamma = 10^{-3}$  meV. (b): As in (a) with  $g = 2.26^{19}$ .

Table II. Comparison between exchange and DM-type anisotropy exchange anisotropy ( $\tilde{\gamma} > 0$ )

	exchange anisotropy ( $\tilde{\gamma} > 0$ )	DM-type anisotropy ( $\gamma \neq 0$ )
$H_{\text{lin}} = 0$	$-\mu_0\eta - 2\tilde{\gamma}\eta + \eta(2v_0\tilde{n} + v_0n_0) = 0$ Two cases: $\eta = 0$ (non-condensed phase) and $\eta \neq 0$ (condensed phase)	$-\mu_0\eta - \gamma + \eta(2v_0\tilde{n} + v_0n_0) = 0$ always condensed magnons, $\eta \neq 0$
Phase transition	$n_c = \frac{\mu_0}{2v_0} + \frac{\tilde{\gamma}}{v_0}$	no phase transition
non-condensed phase	$E_{\mathbf{k}} = \sqrt{(\epsilon_{\mathbf{k}} - \mu_0 + 2\tilde{n}v_0)^2 - 4\tilde{\gamma}^2}$	—————
condensed phase	$E_{\mathbf{k}} = \sqrt{(\epsilon_{\mathbf{k}} + 2\tilde{\gamma})^2 + 2(\epsilon_{\mathbf{k}} + 4\tilde{\gamma})v_0n_0 - 4\tilde{\gamma}^2}$	$E_{\mathbf{k}} = \sqrt{\left(\epsilon_{\mathbf{k}} + \frac{ \gamma }{\sqrt{n_0}}\right)^2 + 2\left(\epsilon_{\mathbf{k}} + \frac{ \gamma }{\sqrt{n_0}}\right)v_0n_0}$

for  $H \perp (10\bar{2})^{19}$  in Fig. 5b. As for  $H \parallel b$  the magnetisation curves show only a smooth increase at temperatures below the minima and no sharp phase transition. Therefore a component of  $\mathbf{D} \perp H$  seems to exist also for this configuration. This could be possibly explained by small lattice distortions leading to domains with different orientation of  $\mathbf{D}$ . In this case a component  $\mathbf{D} \perp H$  could exist for each field configuration. The theoretically calculated  $M(T)$  show reasonable agreement with experiment also for  $H \perp (10\bar{2})$  if we change the  $g$ -factor from 2.06 to 2.26 according to ESR<sup>19,20</sup>. This shows that the variation in  $\gamma$  with field direction and also additional crystal field anisotropies seems to be relatively minor. Although we could certainly improve agreement with experiment by including such effects we have not done so because the number of fit-parameters would be too large.

In Fig. 6a we show the condensed and the non-condensed density separately for the same parameters as in Fig. 5a. The transition from the condensed to the non-

culated everywhere in a perturbative manner.

Finally, we show in Fig. 6b the quasiparticle gap  $\Delta_{qp}$ . As a function of temperature  $\Delta_{qp}$  has a minimum basically at the same point where also the magnetisation curves in Fig. 5a have their minima. The theoretically calculated  $\Delta_{qp}$  as a function of magnetic field at fixed temperature does qualitatively agree with recent ESR measurements<sup>20</sup>. Quantitatively the gap predicted by our theory is about a factor 2 smaller than the one measured by ESR for  $H \parallel b$  at  $H = 9$  T. Two explanations are possible: First, within our theory it is also possible to obtain reasonable agreement with the measured magnetisation curves for  $\gamma \sim 5 \cdot 10^{-3}$  meV by changing  $v_0$  and the excitation gap  $\Delta$  accordingly. In this case  $\Delta_{qp} \sim 0.2$  meV in agreement with ESR. Second and more important, it is not clear if the gap measured in ESR is the pure quasiparticle gap. Within our theory we would expect the gap measured in ESR at fields above the “critical field” (minimum in the gap function) to be given by a combination of one- and two-magnon excitations. In this case the ESR gap would be a combination of the real quasiparticle gap  $\Delta_{qp}$  and  $2\Delta_{qp}$ <sup>24</sup>. To avoid these ambiguities INS measurements of the gap are desirable.

## 5. Specific Heat

To calculate the specific heat  $C_V(H)$  we need the energy  $E_+(H)$  of the lowest triplet component ( $\alpha = +$ ) in the presence of a DMA  $\gamma$  and a magnetic field  $H$ . From Eq. 9 and table II one easily finds

$$E_+(H) = \mu_0 n_0 - (\tilde{n} + n_0)v_0 - \frac{3}{2}v_0 n_0^2 - 4v_0 \tilde{n} n_0 \quad (13)$$

$$- v_0 \tilde{n}^2 + \frac{1}{2N} \sum_{\mathbf{k}} (E_{\mathbf{k}} - \epsilon_{\mathbf{k}}) + \frac{1}{N} \sum_{\mathbf{k}} E_{\mathbf{k}} \tilde{n}_{\mathbf{k}} + \frac{\mu_0}{2}$$

where  $\gamma$  only enters by the condition for the vanishing of the linear term (see table II). As we want to calculate the specific heat for temperatures  $T \sim \Delta$  we also have to take into account the contribution of the triplet mode  $\alpha = 0$ . At  $H = 0$  all modes are of the same importance and the DMA yields only tiny corrections which we can ignore. Therefore the energy  $E(0)$  at zero field of each triplet mode  $\alpha = +, -, 0$  is simply given by

$$E(0) = -2v_0 \tilde{n}^2 + \frac{1}{N} \sum_{\mathbf{k}} (\Omega_{\mathbf{k}0} + 4v_0 \tilde{n}) \tilde{n}_{\mathbf{k}}^0 \quad (14)$$

$$\tilde{n}_{\mathbf{k}}^0 = 1/(\exp[\beta(\Omega_{\mathbf{k}0} + 4v_0 \tilde{n})] - 1).$$

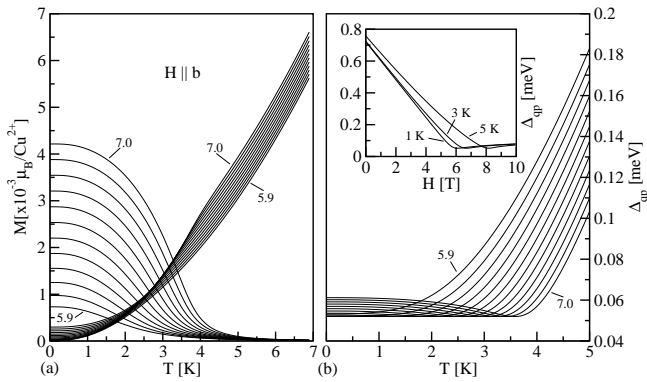


Fig. 6. (a) Condensed and non-condensed magnon densities. (b)  $\Delta_{qp}$  as function of  $T$  for different  $H$  and as function of  $H$  for  $T = 1$  K, 3 K and 5 K (inset). The parameters are as in Fig. 5a.

condensed phase is smeared to a crossover in a region  $\sim 1 - 2$  K around the former transition point. Analytically we find that the temperature region  $\Delta T$  where the densities with  $\gamma \neq 0$  deviate significantly from those without such an anisotropy is given by  $\Delta T/T \sim (\gamma/v_0)^{2/3}/n$ .

As the temperature range where quantum fluctuations are important is much smaller according to Eq. (10) the HFPA is parametrically justified here even in the crossover region. This does not mean that corrections to the HFPA do not exist but these corrections can be cal-

As phonons yield a large contribution to the specific heat which we do not want to consider here, we only compare theoretical and experimental results for  $C_V(H) - C_V(0)$ . In this quantity most phonon contributions should be eliminated. As the  $\alpha = 0$  mode is basically unaffected by the magnetic field we find

$$C_V(H) - C_V(0) = \frac{\partial [E_+(H) - 2E(0)]}{\partial T}. \quad (15)$$

The results are shown in Fig. 7a in comparison to the experimental data<sup>21</sup>. The agreement is good. The overes-

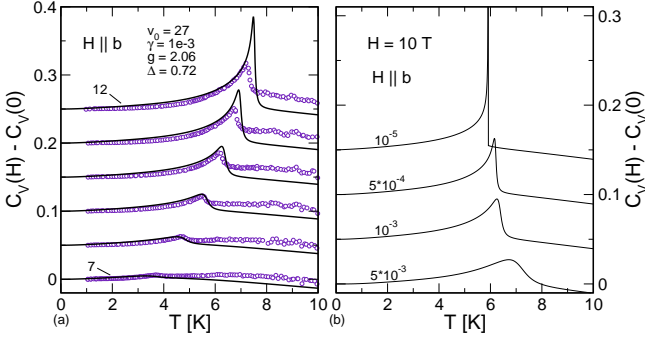


Fig. 7. (a) Measured specific heat<sup>21</sup> (per copper ion) for  $H = 7, 8, \dots, 12$  T (circles) and theoretically calculated (lines). (b) Calculated specific heat for DMA  $\gamma = 5 \cdot 10^{-3}, \dots, 10^{-5}$ . In both graphs the subsequent curves are shifted by 0.05.

timation of the peak heights and slight underestimation of the widths indicates that  $\gamma$  seems to be slightly larger than assumed here. In addition we also see some deviations at higher temperatures particularly at higher fields. Here we should remember that at such energies we have to use in principle the energy and momentum dependent scattering amplitude  $\Gamma(\mathbf{K})$  instead of the constant  $v_0$ . The dependence of peak height and width on  $\gamma$  is shown in Fig. 7b. By increasing  $\gamma$  the peak gets smaller and broader. Note that without anisotropy there would be a singularity in  $C_V(H) - C_V(0)$  at the critical point due to the failure of the HFPA.

## 6. Conclusions

To summarise, we have shown how to incorporate the hard-core constraint into the BO formalism if the magnons are dilute. For  $\text{TiCuCl}_3$  we have found that the dispersion is only slightly modified when compared to<sup>9</sup> where the constraint has been completely ignored. This is due to the following facts: (a) The quasiparticle residue and the self-energies turn out to be almost momentum independent and (b) a fit to the measured dispersion is performed. However, even in this case the correct treatment of the constraint is important when calculating the magnon-magnon scattering amplitude  $v_0$ . We have solved the hard-core boson model using the HFPA and have shown that this approximation is valid apart from a small region around the critical point. Even if  $\text{TiCuCl}_3$  is assumed to be a system without anisotropies no power law  $n_c \sim T^\phi$  can be expected in the exper-

imental temperature range<sup>3</sup> because the quadratic approximation for the dispersion works only for  $T < 1$  K. Next, we have discussed how tiny EA or DMA influence BEC. An EA yields only a small shift in  $n_c$  and a small quasiparticle gap in the condensed phase but leaves the shape of the magnetisation curves otherwise unchanged. On the other hand a DMA has a dramatic effect and smears out the phase transition to a crossover. The different effects of these anisotropies can be understood by the symmetries of the system. With a DMA  $\gamma = 10^{-3}$  meV we have achieved good agreement with experimental data for  $M(T)$  and  $C_V(H, T)$  if  $H \parallel b$ . When rescaled by the  $g$ -factor the agreement with  $M(T)$  for  $H \perp (10\bar{2})$  was also reasonable. This shows that a component of the DM-vector  $\mathbf{D} \perp \mathbf{H}$  seems to exist for each field configuration and that additional crystal field anisotropies are relatively minor. Within our theory we expect a quasiparticle gap  $\Delta_{qp} \sim 0.1$  meV for  $H \parallel b$ ,  $H \sim 10$  T which might be tested in the future.

## Acknowledgment

The authors thank Ch. Rüegg for providing the INS-data and acknowledge support by the ARC. JS acknowledges valuable discussions with M. Oshikawa and I. Affleck and support by the DFG.

- 1) AFFLECK I., *Phys. Rev. B*, **43** (1990) 3215
- 2) GIAMARCHI T. and TSVELIK A. M., *Phys. Rev. B*, **59** (1998) 11398
- 3) NIKUNI T., OSHIKAWA M., OOSAWA A., and TANAKA H., *Phys. Rev. Lett.*, **84** (2000) 5868
- 4) CHUBUKOV A. V., *JETP Lett.*, **49** (1989)
- 5) SACHDEV S. and BHATT R., *Phys. Rev. B*, **41** (1990) 9323
- 6) KOTOV V. N., SUSHKOV O., WEIHONG Z., and OITMAA J., *Phys. Rev. Lett.*, **80** (1998) 5790
- 7) WALECKA J. D. and FETTER A. L., *Quantum theory of many-particle systems* (McGraw Hill College Div., 1971)
- 8) FOR A REVIEW SEE: H. SHI and GRIFFIN A., *Phys. Reports*, **304** (1998) 1
- 9) MATSUMOTO M., NORMAND B., RICE T. M., and SIGRIST M., *Phys. Rev. Lett.*, **89** (2002) 077203
- 10) MATSUMOTO M., NORMAND B., RICE T. M., and SIGRIST M., *Phys. Rev. B*, **69** (2004) 054423
- 11) CAVADINI N., *et al.*, *Phys. Rev. B*, **63** (2001) 172414
- 12) CAVADINI N., *et al.*, *J. Phys. Cond. Mat.*, **12** (2000) 5463
- 13) CHOI K. Y., *et al.*, *Phys. Rev. B*, **68** (2003) 174412
- 14) SHERMAN E. Y., *et al.*, *Phys. Rev. Lett.*, **91** (2003) 057201
- 15) SIRKER J., WEISSE A., and SUSHKOV O. P., *cond-mat/0403311*, (2004)
- 16) SIRKER J., WEISSE A., and SUSHKOV O. P., *cond-mat/0406262*, (2004)
- 17) SAHA-DASGUPTA T. and VALENTI R., *Europhys. Lett.*, **60** (2003) 309
- 18) MISGUICH G. and OSHIKAWA M., *cond-mat/0405422*, (2004)
- 19) OOSAWA A., ISHII M., and TANAKA H., *J. Phys. Cond Mat.*, **11** (1999) 265
- 20) GLAZKOV V. N., SMIRNOV A. I., TANAKA H., and OOSAWA A., *Phys. Rev. B*, **69** (2004) 184410
- 21) OOSAWA A., KATORI H. A., and TANAKA H., *Phys. Rev. B*, **63** (2001) 134416
- 22) WESSEL S., OLSHANII M., and HAAS S., *Phys. Rev. Lett.*, **87** (2001) 206407
- 23) BLAYM G., *et al.*, *Phys. Rev. Lett.*, **83** (1999) 1703
- 24) Details will be published elsewhere